Control System Design for a Rapid Thermal Processing System

Ching-An Lin and Yaw-Kuen Jan

***Abstract*—This paper proposes a control system design for a rapid thermal processing (RTP) system, which has four circular concentric lamp zones and four temperature sensors. The control system consists of a least square feedforward controller and an output feedback proportional plus integral (PI) controller. The goal is to maintain uniform temperature tracking for typical ramp-up and hold-steady profiles. A high-order nonlinear model describing the temperature dynamics of the rapid thermal processing (RTP) system is used for the feedforward controller design. A balanced reduced model, obtained from a linear model around a desired uniform steady-state temperature, is used for the design of the multiinput–multioutput (MIMO) PI controller. The PI controller gain matrices are designed using an LQR-based procedure. Tradeoff between robustness and performance of the system is discussed. Simulation results show the control system designed yields robust temperature tracking with good uniformity for a wide temperature range.**

***Index Terms*—Output feedback, proportional plus integral (PI) controller, rapid thermal processing (RTP), reduced order system, single-wafer process, temperature control, temperature measurement.**

I. Introduction

RAPID thermal processing (RTP) is a relatively new manufacturing technology that is applied in the processing of silicon and gallium arsenide wafers [1], [2]. Maintaining wafer temperature uniformity while following fast temperature trajectories is a key requirement for RTP systems. Many approaches have been proposed for temperature control system design. For example, internal model control with gain-scheduling proposed by Schaper *et al.* [3]–[5], the quadratic dynamic matrix control (QDMC) strategy with successive linearization proposed by Stuber *et al.* [6], closed-loop adaptive control [7], decentralized control [8], and control by iterative learning [9]. It is generally agreed that multizone multisensor feedback control is necessary to meet the stringent uniformity requirement especially when the wafer becomes bigger. For real-time implementation, it is also very desirable to have a simple controller that is not too difficult to tune. The decentralized control with steady-state model proposed in [8] can be viewed as an effort in this direction.

This paper proposes a control system design method for an RTP system with four concentric lamp zones. The control system consists of a feedforward least square open-loop controller and a simple proportional integral (PI) feedback controller. One of the advantages of a PI controller is its simplicity: the controller order equals to the sensor number. It is also suitable for ramp-up and hold-steady temperature commands typical for RTP processes. The proposed design method involves establishing a model based on the uniform steady state, model reduction via balanced realization, and an LQR design for choosing the gain matrices. Robustness of the design is guaranteed by imposing a constraint, based on model reduction error, on the design requirement. Design tradeoff between dynamic performance and robustness is achieved by choosing the parameters in the LQR performance index. The controller designed is simple and the PI gain matrices can be easily tuned. Simulation results show that the control system designed yields robust temperature tracking with good uniformity over a wide range of temperature.

We consider an RTP system which has a circular chamber and four concentric lamp zones. A simplified schematic of the RTP system is shown in Fig. 1 [10]. The lamp configuration has been optimally designed for maintaining uniform temperature on the wafer. A detailed design procedure can be found in [10].

By dividing the wafer into N concentric zones, starting from the center, and assuming that the temperature and the radiosity over each zone are uniform, we obtain a high-order nonlinear state equation in matrix form

$$\begin{bmatrix} \dot{T}_1 \\ \vdots \\ \dot{T}_N \end{bmatrix} = \mathbf{D} \begin{bmatrix} T_1 \\ \vdots \\ T_N \end{bmatrix} + \mathbf{E} \begin{bmatrix} T_1^4 \\ \vdots \\ T_N^4 \end{bmatrix} + \mathbf{F} \begin{bmatrix} B_1 \\ \vdots \\ B_4 \end{bmatrix} + \mathbf{V} \left(\begin{bmatrix} T_{\infty 1} \\ \vdots \\ T_{\infty N} \end{bmatrix} - \begin{bmatrix} T_1 \\ \vdots \\ T_N \end{bmatrix} \right) \quad (1.1)$$

where $T_i, i = 1,2,\ldots,N-1$, denotes the temperature of the ith wafer zone, and T_N is the temperature of wafer edge, $B_j, j = 1,\ldots,4$, is the heat flux generated by the jth lamp, $T_{\infty i}, i = 1,2,\ldots,N$, is the ambient temperature of the ith wafer zone, matrix $\mathbf{D}$ describes the effect of conduction, matrices $\mathbf{E}$ and $\mathbf{F}$ describe the effect of radiation including reflection of the chamber wall, and matrix $\mathbf{V}$ describes the convective heat transfer. A detailed derivation of (1.1) can be found in [11]. These matrices depend on the distribution of wafer temperature. In the design example, we take $N = 101$ for a 200-mm wafer.

This paper is organized as follows. Section II describes the control system structure. Section III establishes the relation between sensor locations and steady-state performance and proposes a method to determine good sensor locations. Section IV

Manuscript received January 1, 1999; revised June 9, 2000. Recommended by Associate Editor, S. Nair. This work was supported by National Science Council under Grant NSC-88-2218-E009-005.

The authors are with the Department of Electrical and Control Engineering, National Chiao-Tung University, Hsinchu, Taiwan, R.O.C. (e-mail: calin@cc.nctu.edu.tw; ykjan@ms32.hinet.net).

Publisher Item Identifier S 1063-6536(00)00517-0.

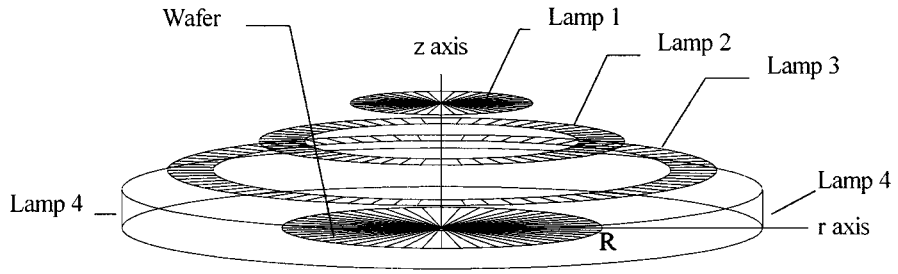

Fig. 1. A simplified schematic of the RTP system.

discusses the design of PI controller gain matrices. Design procedure and simulation results are given in Section V. Section VI provides a brief conclusion.

II. Control System Structure

The block diagram of the proposed control system is shown in Fig. 2. We use the open-loop feedforward control law proposed in [10], that is

$$\begin{bmatrix} B_{1o}(t) \\ \vdots \\ B_{4o}(t) \end{bmatrix} = (\mathbf{F}^T\mathbf{F})^{-1}\mathbf{F}^T \left\{ \begin{bmatrix} \dot{T}_d(t) \\ \vdots \\ \dot{T}_d(t) \end{bmatrix} - \mathbf{E} \begin{bmatrix} T_d(t)^4 \\ \vdots \\ T_d(t)^4 \end{bmatrix} \right\} \tag{2.1}$$

where $T_d(t)$ is the desired temperature trajectory. As seen in [10], a criterion for choosing a lamp configuration, which determines $\mathbf{F}$, is to make the equation error

$$\delta(t) = \begin{bmatrix} \dot{T}_d(t) \\ \vdots \\ \dot{T}_d(t) \end{bmatrix} - \mathbf{E} \begin{bmatrix} T_d(t)^4 \\ \vdots \\ T_d(t)^4 \end{bmatrix} - \mathbf{F} \begin{bmatrix} B_{1o}(t) \\ \vdots \\ B_{4o}(t) \end{bmatrix} \tag{2.2}$$

small. To make the equations compact, we also define the following variables:

$$u(t) := \begin{bmatrix} B_1(t) \\ \vdots \\ B_4(t) \end{bmatrix}, \quad x(t) := \begin{bmatrix} T_1(t) \\ \vdots \\ T_N(t) \end{bmatrix},$$

$$x_\infty(t) := \begin{bmatrix} T_{\infty,1}(t) \\ \vdots \\ T_{\infty,N}(t) \end{bmatrix}, \quad z(t) := \begin{bmatrix} T_1(t)^4 \\ \vdots \\ T_N(t)^4 \end{bmatrix},$$

$$x_d(t) := \begin{bmatrix} T_d(t) \\ \vdots \\ T_d(t) \end{bmatrix} \in R^N, \quad \text{and}$$

$$z_d(t) := \begin{bmatrix} T_d(t)^4 \\ \vdots \\ T_d(t)^4 \end{bmatrix} \in R^N$$

in Fig. 2. The control input $u(t)$ is the sum of the open-loop control $u_o(t)$, defined in (2.1), and an additional input $\tilde{u}(t)$ (to be provided by feedback), i.e.,

$$u(t) = u_o(t) + \tilde{u}(t).$$

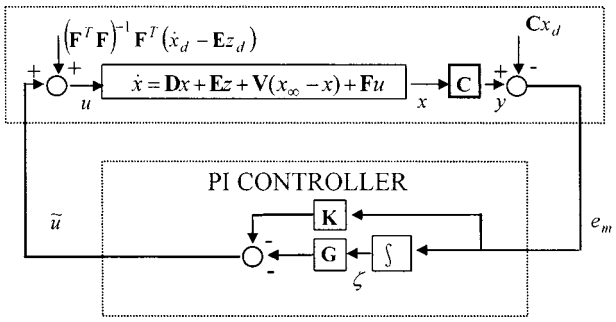

Fig. 2. The RTP system with feedforward and PI feedback control.

We measure the wafer temperature at four points (zones). Thus the measured output is

$$y(t) = \mathbf{C}x(t)$$

where $\mathbf{C}$ is a $4 \times N$ matrix with all zero entries except a one in each row indicating the measurement location. Let $e_m(t) := y(t) - \mathbf{C}x_d(t)$ be the temperature error at the measured locations. Thus

$$e_m(t) = \mathbf{C}e(t). \tag{2.3}$$

The PI controller is described by

$$\begin{cases} \dot{\zeta}(t) = e_m(t) \\ \tilde{u}(t) = -\mathbf{G}\zeta(t) - \mathbf{K}e_m(t) \end{cases} \tag{2.4}$$

where the constant matrices $\mathbf{K}$ and $\mathbf{G}$ are proportional gain and integral gain, respectively, to be designed.

Let $e(t) := x(t) - x_d(t)$ be the temperature error vector. From (1.1) and (2.2), the equation describing the dynamics of $e(t)$ is

$$\dot{e}(t) = \mathbf{A}e(t) + \mathbf{F}\tilde{u}(t) + w(t) \tag{2.5}$$

where we have (2.6)–(2.8), shown at the bottom of the next page. Typical desired temperature trajectory $T_d(t)$ in many RTP applications can be characterized as a ramp at a constant positive slope followed by a hold [3]. Since the matrices $\mathbf{D}, \mathbf{E}, \mathbf{F}$, and $\mathbf{V}$ in (1.1) and hence (2.2) depend only on the temperature of the wafer, if the wafer temperature has uniformly reached the desired steady state, that is, the final value of $T_d(t)$, then these matrices become constant. Hence, in the sequel we will take them as constant matrices corresponding to a specified steady-state (final) value of $T_d(t)$. To simplify further, we take $\tilde{\mathbf{E}} = 4T_d(t_f)^3\mathbf{E}$ where $T_d(t_f)$ is the final value of $T_d(t)$.

Thus (2.5) gives a linear time-invariant model for the dynamics of the RTP system, where $w(t)$ is the disturbance term which takes the convection effect into account. This is the model we will use in the design of sensor locations and the PI controller. Later in simulations, to verify the design, the nonlinear high-order model (1.1) will be used.

Combining (2.3) through (2.5), the dynamic model of the closed-loop system is

$$\begin{bmatrix} \dot{e}(t) \\ \dot{\zeta}(t) \end{bmatrix} = \mathbf{A}_{\text{cl}} \begin{bmatrix} e(t) \\ \zeta(t) \end{bmatrix} + \begin{bmatrix} w(t) \\ \mathbf{O} \end{bmatrix} \tag{2.9}$$

where

$$\mathbf{A}_{\text{cl}} := \begin{bmatrix} \mathbf{A} - \mathbf{FKC} & -\mathbf{FG} \\ \mathbf{C} & \mathbf{O}_{4\times 4} \end{bmatrix}. \tag{2.10}$$

III. Sensor Locations and Steady-State Performance

In this section we show that as long as the closed-loop system is stable, the steady-state temperature error is completely determined by the sensor locations and we propose a method to choose good sensor locations. Thus the subsequent design of the gain matrices $\mathbf{K}$ and $\mathbf{G}$ would not affect the steady-state performance.

Consider the closed-loop RTP system (2.9). Suppose the matrices $\mathbf{K}$ and $\mathbf{G}$ have been chosen so that the system is stable.[1] Assume that the disturbance $w(t) \to w_\infty$, a constant vector, as $t \to \infty$. We note that in view of (2.8) and (2.2), this assumption is equivalent to that the ambient temperature $x_\infty(t)$ approaches constant steady state as $t \to \infty$.

We note first that closed-loop stability implies that $\mathbf{A}_{\text{cl}}$, in (2.10), is nonsingular, which in turn implies that $\mathbf{G}$, the integral gain matrix, is nonsingular. It is intuitively clear that $\mathbf{G}$ must be nonsingular, otherwise a linear combination of the integrator states would be unstable and unobservable. Let $e_s = \lim_{t\to\infty} e(t)$ and $\tilde{u}_s = \lim_{t\to\infty} \tilde{u}(t)$. From (2.5) and (2.4), we have

$$\mathbf{A}e_s + \mathbf{F}\tilde{u}_s + w_\infty = \mathbf{O} \quad \text{and} \quad \mathbf{C}e_s = \mathbf{O}. \tag{3.1}$$

It then follows that the closed-loop steady-state temperature error is given by

$$e_s = \left(\mathbf{I}_N - \mathbf{A}^{-1}\mathbf{F}(\mathbf{CA}^{-1}\mathbf{F})^{-1}\mathbf{C}\right)\alpha \tag{3.2}$$

[1]We will use "stable" to mean "asymptotically stable."

where $\alpha = -\mathbf{A}^{-1}w_\infty$, provided that $\mathbf{CA}^{-1}\mathbf{F}$ is nonsingular. We note that, from (2.5), α is the open-loop steady-state temperature error and that $\mathbf{CA}^{-1}\mathbf{F}$ is nonsingular means that the RTP system has no transmission zero at dc. Since $\mathbf{A}, \mathbf{F}$, and α are fixed, the steady-state error e_s is completely determined by $\mathbf{C}$ and is independent of $\mathbf{K}$ and $\mathbf{G}$. Let $\mathbf{J} = [J_1\ J_2\ J_3\ J_4], 1 \le J_1 < J_2 < J_3 < J_4 \le N$, be the location indexes of wafer temperature to be measured. A criterion to choose $\mathbf{J}$, and hence $\mathbf{C}$, is to make $\|e_s\|_\infty \ll \|\alpha\|_\infty$, where $\|\cdot\|_\infty$ denotes the infinite norm of a vector.

Let $\hat{\mathbf{F}}_j$ denote the jth row of $\mathbf{A}^{-1}\mathbf{F}$. Then $\hat{\mathbf{F}}_{j_i}, i = 1,2,3,4$, is the ith row of $\mathbf{CA}^{-1}\mathbf{F}$. We think of the jth row of $\mathbf{A}^{-1}\mathbf{F}(\mathbf{CA}^{-1}\mathbf{F})^{-1}$ as the coefficients of $\hat{\mathbf{F}}_j$ expressed as a linear combination of $\hat{\mathbf{F}}_{j_i}, i = 1,2,3,4$. Therefore, from (3.2), if $\hat{\mathbf{F}}_j, J_i \le j \le J_{i+1}$, satisfies

$$\hat{\mathbf{F}}_j = \frac{j - J_i}{J_{i+1} - J_i}\hat{\mathbf{F}}_{J_{i+1}} + \frac{J_{i+1} - j}{J_{i+1} - J_i}\hat{\mathbf{F}}_{J_i} \tag{3.3}$$

then the jth entry of e_s in (3.2) satisfies

$$e_{sj} = \alpha_j - \left(\frac{j - J_i}{J_{i+1} - J_i}\alpha_{J_{i+1}} + \frac{J_{i+1} - j}{J_{i+1} - J_i}\alpha_{J_i}\right). \tag{3.4}$$

This means that if one row of $\mathbf{A}^{-1}\mathbf{F}$ is interpolated from j_ith and J_{i+1}th rows of $\mathbf{A}^{-1}\mathbf{F}$, then the corresponding entry of the closed-loop steady-state error is the deviation of corresponding entry of α from a value interpolated accordingly from J_ith and J_{i+1}th entries of α. This generally has the effect of making the curve of e_s smoother than that of α. The proposed method of choosing $J_i, i = 1,2,3,4$, is as follows. First, let $\mathbf{F}_i$ be the ith column of $\mathbf{F}$ and plot $\mathbf{A}^{-1}\mathbf{F}_i, i = 1,2,3,4$, with respect to entry index $j, j = 1,\ldots,N$. Second, let $J_1 = 1, J_4 = N$ and find indexes J_2 and J_3 to separate these curves so that all broken segments between each two neighboring indexes are nearly straight. These indexes $J_i, i = 1,2,3,4$, are then collected as $\mathbf{J}$ if the resultant matrix $\mathbf{CA}^{-1}\mathbf{F}$ is nonsingular. This approach is especially suitable when the associated broken segments of α are also nearly straight, as will be seen from the example in Section V.

IV. Design of Gain Matrices Based on a Reduced Model

In this section we propose an LQR-based method for designing the gain matrices $\mathbf{K}$ and $\mathbf{G}$. We first obtain a reduced-order model from the high-order linear system (2.5) and (2.3) via balanced realization [12]. The design problem is cast as an

---

$$\mathbf{A} = \mathbf{D} - \mathbf{V} + \tilde{\mathbf{E}}, \tag{2.6}$$

$$\tilde{\mathbf{E}} = \mathbf{E}\begin{bmatrix} \left(T_1(t)^2 + T_d(t)^2\right)\left(T_1(t) + T_d(t)\right) & 0 \cdots & 0 \\ 0 & \ddots\ \ddots & \vdots \\ \vdots & \ddots\ \ddots & 0 \\ 0 & \cdots\ 0 & \left(T_N(t)^2 + T_d(t)^2\right)\left(T_N(t) + T_d(t)\right) \end{bmatrix} \tag{2.7}$$

and

$$w(t) = \mathbf{V}(x_\infty(t) - x_d(t)) - \delta(t). \tag{2.8}$$

optimal LQR state feedback problem. Design parameters are included in the quadratic performance index to allow tradeoffs between speed of response and robustness.

A. Reduced Order Model and Robustness Condition

Consider the open-loop controlled RTP system described by (2.5) and (2.3). The system is stable and, with the disturbance $w(t)$ neglected, is described by

$$\begin{cases} \dot{e}(t) = \mathbf{A}e(t) + \mathbf{F}\tilde{u}(t) \\ e_m(t) = \mathbf{C}e(t) \end{cases}. \tag{4.1}$$

The corresponding transfer matrix is $H(s) = \mathbf{C}(s\mathbf{I} - \mathbf{A})^{-1}\mathbf{F}$.

Let $\sigma_1 \geq \sigma_2 \geq \cdots \geq \sigma_r > \sigma_{r+1} \geq \sigma_{r+2} \geq \cdots \geq \sigma_N > 0$ be the Hankel singular values of the system (4.1) [12]. Let the reduced-order system obtained from (4.1) via balanced realization, by keeping r states, be

$$\begin{cases} \dot{\bar{e}}(t) = \bar{\mathbf{A}}_{11}\bar{e}(t) + \bar{\mathbf{F}}_1\bar{u}(t) \\ \bar{e}_m(t) = \bar{\mathbf{C}}_1\bar{e}_t \end{cases} \tag{4.2}$$

where $\bar{e}(t), \bar{u}(t)$ and $\bar{e}_m(t)$ are the state, input, and output, respectively. The reduced-order system is stable with transfer matrix $H_r(s) = \bar{\mathbf{C}}_1(s\mathbf{I} - \bar{\mathbf{A}}_{11})^{-1}\bar{\mathbf{F}}_1$. It is well known that the model reduction error satisfies [12]

$$\|H - H_r\|_\infty \leq 2\sum_{i=r+1}^{N} \sigma_i \tag{4.3}$$

where $\|H\|_\infty := \sup_{\varpi \in R} \bar{\sigma}(H(j\varpi))$.

Consider now the PI controller for the reduced-order system (4.2) defined by the state equation

$$\begin{cases} \dot{\bar{\zeta}}(t) = \bar{e}_m(t) \\ \bar{u}(t) = -\mathbf{G}\bar{\zeta}(t) - \mathbf{K}\bar{e}_m(t) \end{cases} \tag{4.4}$$

where $\bar{\zeta}(t)$ is the state of the controller. If the closed-loop system described by (4.2) and (4.4) is stable, then the closed-loop system with the original plant (4.1) and the same controller ($\mathbf{K}$ and $\mathbf{G}$) would be stable, provided [13]

$$\|Q\|_\infty < \frac{1}{2\sum_{i=r+1}^{N} \sigma_i} \tag{4.5}$$

where

$$Q(s) = -\left[\mathbf{I} + \left(\mathbf{G}\frac{\mathbf{1}}{s} + \mathbf{K}\right) H_r(s)\right]^{-1} \left(\mathbf{G}\frac{1}{s} + \mathbf{K}\right).$$

B. Design of K and G

We now consider the design of $\mathbf{K}$ and $\mathbf{G}$. If we take $\left[\begin{smallmatrix} \bar{e}(t) \\ \bar{\zeta}(t) \end{smallmatrix}\right]$ as the state of the closed-loop system (4.2) and (4.4), the equation can be written in state feedback form. More precisely, we have

$$\begin{bmatrix} \dot{\bar{e}}(t) \\ \dot{\bar{\zeta}}(t) \end{bmatrix} = (\mathbf{A}_r - \mathbf{B}_r\mathbf{K}_r) \begin{bmatrix} \bar{e}(t) \\ \bar{\zeta}(t) \end{bmatrix} \quad \text{and}$$
$$\bar{u}(t) = -\mathbf{K}_r \begin{bmatrix} \bar{e} \\ \bar{\zeta} \end{bmatrix}$$

where

$$\mathbf{A}_r = \begin{bmatrix} \bar{\mathbf{A}}_{11} & \mathbf{O}_{r\times 4} \\ \bar{\mathbf{C}}_1 & \mathbf{O}_{4\times 4} \end{bmatrix}, \quad \mathbf{B}_r = \begin{bmatrix} \bar{F}_1 \\ \mathbf{O}_{4\times 4} \end{bmatrix} \quad \text{and}$$
$$\mathbf{K}_r = [\mathbf{K}\bar{\mathbf{C}}_1 \ \mathbf{G}].$$

Let the LQR cost function be

$$\int_0^\infty \left\{ \begin{bmatrix} \bar{e}(t) \\ \bar{\zeta}(t) \end{bmatrix}^T \begin{bmatrix} \eta^2\bar{\mathbf{C}}_1^T\bar{\mathbf{C}}_1 & \mathbf{O}_{r\times 4} \\ \mathbf{O}_{4\times r} & \lambda^2\mathbf{I}_4 \end{bmatrix} \begin{bmatrix} \bar{e}(t) \\ \bar{\zeta}(t) \end{bmatrix} + \|\bar{u}(t)\|_2^2 \right\} dt \tag{4.6}$$

where η and λ are weighting parameters to be adjusted to meet transient and robustness requirements. For each η and λ, there corresponds an optimal control law

$$\bar{u}(t) = -\mathbf{K}^* \begin{bmatrix} \bar{e}(t) \\ \bar{\zeta}(t) \end{bmatrix}$$

which minimizes (4.6). The unique state feedback gain matrix $\mathbf{K}^*$ can be computed by solving a matrix algebraic Riccati equation [14]. Since $\mathbf{A}_r - \mathbf{B}_r\mathbf{K}^*$ is stable [14], $\mathbf{A}_{\text{cr}}$ is stable if there exist $\mathbf{K}$ and $\mathbf{G}$ such that $\mathbf{K}_r = \mathbf{K}^*$. And this is true if $\bar{\mathbf{C}}_1$ is square and nonsingular, since we can set $\mathbf{K} = \mathbf{K}_1^*\bar{\mathbf{C}}_1^{-1}$ and $\mathbf{G} = \mathbf{K}_2^*$ where $\mathbf{K}^* = [\mathbf{K}_1^* \ \mathbf{K}_2^*]$.

If $\bar{\mathbf{C}}_1$ is not square and $\bar{\mathbf{C}}_1\bar{\mathbf{C}}_1^T$ is nonsingular, based on a least square approximation of $\mathbf{K}_r$ to $\mathbf{K}^*$, we let

$$\mathbf{K} = \mathbf{K}_1^*\bar{\mathbf{C}}_1^T\left(\bar{\mathbf{C}}_1\bar{\mathbf{C}}_1^T\right)^{-1} \quad \text{and} \quad \mathbf{G} = \mathbf{K}_2^*. \tag{4.7}$$

Controller gain matrices thus designed will give a property that a performance index $\sum_{i=1}^{4} |\int_0^\infty e_{J_i}(t)\,dt|^2$ of the original system is determined only by the value of the weighting parameter λ. We will prove this in the next section. Suppose the dimension of $\bar{\mathbf{C}}_1$ is $4 \times r$ with $r \geq 4$. The following proposition gives a sufficient condition for $\bar{\mathbf{C}}_1\bar{\mathbf{C}}_1^T$ to be nonsingular. A proof of which can be found in [11].

Proposition 4.1: Let the singular values of the matrix $\mathbf{X} = \mathbf{C}\mathbf{A}^{-1}\mathbf{F}$ be $\hat{\sigma}_i, i = 1,2,3,4$ with $\hat{\sigma}_1 \geq \hat{\sigma}_2 \geq \hat{\sigma}_3 \geq \hat{\sigma}_4$. If $\hat{\sigma}_4 > 2\sum_{i=r+1}^{N} \sigma_i$ then $\bar{\mathbf{C}}_1\bar{\mathbf{C}}_1^T$ is nonsingular. □

For given r, since $\mathbf{K}^*$ is uniquely determined (and thus are $\mathbf{K}$ and $\mathbf{G}$) by the given η and λ, it remains to see how to choose η and λ such that (4.5) is satisfied and the dynamic performance has the desired transient property.

C. Performance Analysis

We will first show that the dynamic performance is closely related to λ, the weighting parameter associated with the integral error. From (3.1), $\tilde{u}_s = -(\mathbf{C}\mathbf{A}^{-1}\mathbf{F})^{-1}\mathbf{C}\mathbf{A}^{-1}w_\infty$ and is independent of $\mathbf{K}$ and $\mathbf{G}$. And we also have

$$\lim_{t\to\infty} \zeta(t) = \left[\int_0^\infty e_{J_1}(t)\,dt \ldots \int_0^\infty e_{J_4}(t)\,dt\right]^T$$
$$= -\mathbf{G}^{-1}\tilde{u}_s \tag{4.8}$$

where $\zeta(t)$ and $e(t)$ are states of the original system (2.9). The dependence of the dynamic performance on λ is described by the following proposition.

Proposition 4.2: Consider the system (2.9). Suppose $\mathbf{G}$ is designed as (4.7). Then

(a) $\mathbf{G}^T\mathbf{G} = \lambda^2\mathbf{I}_4$

(b) $\left\|\lim_{t\to\infty}\zeta(t)\right\|_2^2 = \sum_{i=1}^{4}\left|\int_0^\infty e_{J_i}(t)\,dt\right|^2 = \frac{1}{\lambda^2}\|\tilde{u}_s\|_2^2.$

Proof: Assertion (a) follows from the Riccati equation associated with the LQR problem and (b) follows from (a) and (4.8).

Remark: Condition (b) shows that $\sum_{i=1}^{4}|\int_0^\infty e_{J_i}(t)\,dt|^2$ is inverse proportional to λ^2.

Note that the cost function in (4.6) is equal to

$$\int_0^\infty \left\{\eta^2\|\bar{e}_m(t)\|_2^2 + \lambda^2\|\bar{\zeta}(t)\|_2^2 + \|\bar{u}(t)\|_2^2\right\}\,dt.$$

With such a cost function, small η and λ generally give small $\int_0^\infty \|\bar{u}(t)\|_2^2\,dt$. Since roughly $\|Q\|_\infty$ is the gain from the reference input to the control input $\bar{u}$, small η and λ give small $\|Q\|_\infty$. Hence if λ has been designed large enough to get small $\sum_{i=1}^{4}|\int_0^\infty e_{J_i}(t)\,dt|^2$ and good transient response, we need to reduce η in order to reduce the value of $\|Q\|_\infty$.

To summarize, when sensor locations have been determined, the following conditions are required for stability: 1) $\bar{\mathbf{C}}_1\bar{\mathbf{C}}_1^T$ is nonsingular; 2) $\mathbf{A}_{\rm cr}$ is stable; and 3) (4.5) must be satisfied in designing controller gain matrices. Note that if $\bar{\mathbf{C}}_1$ is square and nonsingular, $\mathbf{A}_{\rm cr}$ is always stable. If $\bar{\mathbf{C}}_1$ is not square, we need to check that $\bar{\mathbf{C}}_1\bar{\mathbf{C}}_1^T$ is nonsingular and the corresponding $\mathbf{A}_{\rm cr}$ is stable. To satisfy condition 3) we should decrease η; to satisfy the requirement on dynamic performance we should increase λ.

V. Design Procedure and Simulation Results

A. Design Procedure

The design procedure for the PI controller is summarized as follows.

Step 1) Use the method proposed in Section III to choose $\mathbf{J}$, the sensor locations.

Step 2) Find the smallest singular value $\hat{\sigma}_4$ of the matrix $\mathbf{CA^{-1}F}$ and perform balanced realization on $H(s)$ to get $\sigma_i, i = 1,\ldots,N$. Let r_0 be the smallest p satisfying $\hat{\sigma}_4 > 2\sum_{i=p+1}^{N}\sigma_i$ and $p \geq 4$. Assign the dimension of the reduced order system as r_0.

Step 3) Extract the reduced order system from the balanced realization of $H(s)$. Choose small η and large λ (with $\lambda \gg \eta$) for the cost function given in (4.6). Assign factors χ_1 and χ_2 with $0 < \chi_1 < \chi_2 \leq 1$.

Step 4) Find the optimal $\mathbf{K}^*$ which minimizes the cost function. Assign gain matrices $\mathbf{K}$ and $\mathbf{G}$ as in (4.7). Compute $\|Q\|_\infty$.

Step 5) Decrease η and repeat Step 4) until the value of $\|Q\|_\infty$ does not change significantly as η decreases.

Step 6) The design is completed if

$$\frac{\chi_1}{2\sum_{i=r+1}^{N}\sigma_i} \leq \|Q\|_\infty < \frac{\chi_2}{2\sum_{i=r+1}^{N}\sigma_i}$$

and $\mathbf{A}_{\rm cr}$ is stable. Otherwise

i) If $\|Q\|_\infty \geq (\chi_2/2\sum_{i=r+1}^{N}\sigma_i)$ then decrease λ and go to Step 4).

ii) If $\|Q\|_\infty < (\chi_1/2\sum_{i=r+1}^{N}\sigma_i)$ then increase λ and go to Step 4).

iii) If $\mathbf{A}_{\rm cr}$ is not stable then increase the dimension of the reduced-order system by one and go to Step 3).

Remark: (a) Note that in Step 3) we assign factors χ_1 and χ_2 to make the adjustment of $\|Q\|_\infty$ stop at a condition of

$$\frac{\chi_1}{2\sum_{i=r+1}^{N}\sigma_i} \leq \|Q\|_\infty < \frac{\chi_2}{2\sum_{i=r+1}^{N}\sigma_i}.$$

(b) In Step 2), the dimension r can be arbitrarily chosen from the integer set $\{r_o, r_{o+1},\ldots,N\}$.

B. Simulation Results

The lamp configuration in [10] is used to simulate the performance of the proposed control system. The simulations for both closed-loop and open-loop controlled systems are based on the high-order nonlinear model with the effect of convection included. The physical parameters of the system under study are the following. 1) The thickness of the 200 mm wafer is 1 mm. The wafer has a total emissivity 0.7 and it is divided into 101 concentric zones. 2) The widths of the ring-type lamps and lamp 4 are fixed at 10 mm and the radius of the disk-type lamp 1 is 25 mm. 3) The radius of the chamber is 180.5 mm and this also is the radius of lamp 4. The height and radius of lamp 3 is 26 mm and 100 mm, respectively. The height and radius of lamp 2 is 87.9 mm and 84.2 mm, respectively. The wall and ceiling of the chamber have an emissivity of 0.5 except for these areas occupied by lamps. The chamber wall and ceiling are totally divided into 49 annular zones. 4) The ambient temperature (°C) of the ith wafer zone is $T_{\infty i} = 300$ for $i = 1, 2,\ldots, 101$. The convective heat coefficient $h_i(r)$ is approximated [15] as $7.1 + 4.3(r_i/R)^4$ (W/m^{2}K).

The tracking error at time t for temperature profile $T_d(t)$ is defined as

$$\max_{1\leq i\leq 101}|T_i(t) - T_d(t)| = \max_{1\leq i\leq 101}|e_i(t)|.$$

The temperature profile (°C) used for the controller design is

$$T_d(t) = \begin{cases} 400 + 100t & \text{for } 0 \leq t < 7 \\ 1100 & \text{for } 7 \leq t \leq 30 \end{cases}. \qquad (5.1)$$

Following the design procedure, four columns of $\mathbf{A}^{-1}\mathbf{F}$ and the computed open-loop steady-state error, α, are plotted in Fig. 3 for choosing $\mathbf{J}$. The computed steady-state tracking error, $\max_{1\leq i\leq 101}|\alpha_i|$, is 19.4492°C. Since the most nonlinear column of $\mathbf{A}^{-1}\mathbf{F}$ is $\mathbf{A}^{-1}\mathbf{F}_3$, approximating $\mathbf{A}^{-1}\mathbf{F}_3$ by a piecewise linear curve is most important. We thus choose $\mathbf{J} = [1\ 55\ 95\ 101]$.

The computed Hankel singular values of $H(s)$ are $2.1076, 0.834, 0.1045, 0.0335, 0.0097, 0.0040, 0.0009\ldots$.
Since $\hat{\sigma}_4 = 0.0482$ and $2\sum_{i=5}^{101}\sigma_i = 0.0307$, $\bar{\mathbf{C}}_1$ is nonsingular

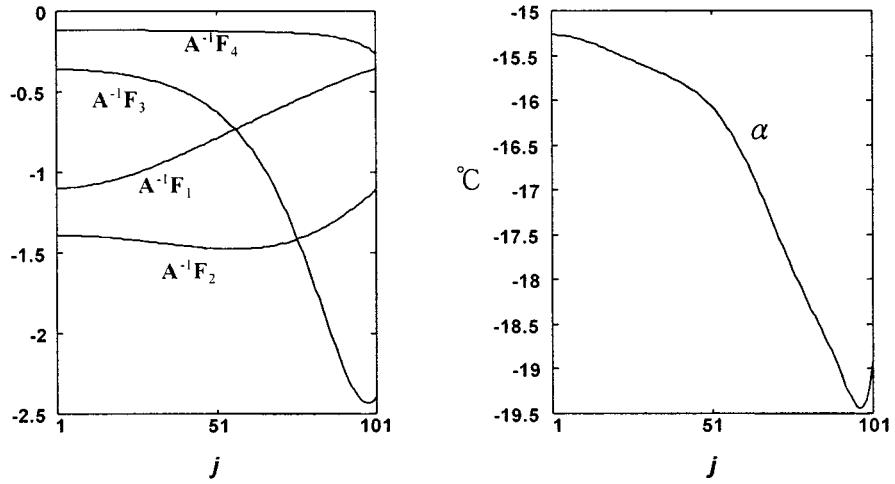

Fig. 3. Four columns of $\mathbf{A}^{-1}\mathbf{F}$ and open-loop steady-state error, α.

TABLE I
SIMULATED RESULTS FOR DIFFERENT TRAJECTORIES WHEN $\mathbf{K}$ AND $\mathbf{G}$ ARE GIVEN IN (5.2)

Hold-heating temp. in simulation	Convection effect included			No convection effect		
	$\max_{t\in[0,30]}\max_{i\in[1,101]}\lvert e_i\rvert$	$\min_{t\in[7,30]}\max_{i\in[1,101]}\lvert e_i\rvert$	$\max_{i\in[1,101]}\lvert e_i\rvert_{t=30}$	$\max_{t\in[0,30]}\max_{i\in[1,101]}\lvert e_i\rvert$	$\min_{t\in[7,30]}\max_{i\in[1,101]}\lvert e_i\rvert$	$\max_{i\in[1,101]}\lvert e_i\rvert_{t=30}$
1100℃	0.554	0.205	0.214	0.578	0.179	0.211
1000℃	0.446	0.153	0.153	0.467	0.133	0.152
1200℃	0.666	0.256	0.290	0.692	0.234	0.284

for $r = 4$. With $\chi_1 = 0.98, \chi_2 = 1$ and (η, λ) starting from $(10, 100)$, the design procedure gives $\eta = 0.007, \lambda = 25.4187$

$$\mathbf{K} = \begin{bmatrix} 21.3418 & -14.0787 & 0.0367 & 0.7650 \\ -5.0963 & 19.5557 & 0.4605 & -0.9626 \\ -0.0002 & -4.9936 & 8.2223 & 3.5416 \\ 0.3644 & 1.5305 & -6.9740 & 6.2981 \end{bmatrix} \quad (5.2a)$$

and

$$\mathbf{G} = \begin{bmatrix} 24.8012 & -5.4934 & 0.6156 & 0.6717 \\ 5.2462 & 24.3557 & 4.9482 & 0.9477 \\ -1.8266 & -4.1358 & 19.2298 & 15.9962 \\ 0.3848 & 2.3714 & -15.8574 & 19.7200 \end{bmatrix} \quad (5.2b)$$

The value of the resultant $\|Q\|_\infty$ is 32.3864, thus $\|Q\|_\infty < (1/2\sum_{i=5}^{101}\sigma_i) = 32.5733$. To demonstrate the robustness of the PI controller (5.2), simulations are performed for three desired temperature trajectories: all start from 400°C but with three hold temperatures 1100°C, 1000°C and 1200°C beginning at $t = 7$. Convection effects considered include $\mathbf{V} = (1/\rho HC)\text{diag}[h_1, h_2, \ldots, h_{101}]$ and $\mathbf{V} = \mathbf{O}$. The results are summarized in Table I which includes $\max_{\substack{1\le i\le 101\\ 0\le t\le 30}}|e_i(t)|$, $\min_{7\le t\le 30}\max_{1\le i\le 101}|e_i(t)|$ and $\max_{i\in[1,101]}|e_i(t)|_{t=30}$. It is clear that $\max_{\substack{1\le i\le 101\\ 0\le t\le 30}}|e_i(t)|$ is the most significant performance index for the temperature controller. The second entry, $\min_{7\le t\le 30}\max_{1\le i\le 101}|e_i(t)|$, represents the damping behavior of the tracking error. The third entry, $\max_{i\in[1,101]}|e_i(t)|_{t=30}$, is used to compare with the computed steady-state tracking error. The maximal tracking error during the entire heating process, $\max_{\substack{1\le i\le 101\\ 0\le t\le 30}}|e_i(t)|$, is less than 0.7°C for all these trajectories. Hence, the controller designed achieves good performance and robustness.

For all these cases, it turns that tracking error at $t = 30$ is very close to the computed steady-state tracking error, $\max_{1\le j\le 101}\lim_{t\to\infty}|e_j(t)|$. When sensor noise is added to the simulation, roughly the same amount of sensor noise propagates to the tracking error.

We next consider a case where $\bar{\mathbf{C}}_1$ is not square. When the dimension of the reduced-order system is increased to six, the design procedure gives $\eta = 0.0417, \lambda = 1710.2$

$$\mathbf{K} = \begin{bmatrix} 194.197 & -136.426 & 9.383 & 0.649 \\ -52.506 & 178.272 & -4.393 & -2.832 \\ 3.085 & -48.618 & 79.492 & 20.838 \\ -2.220 & 23.374 & -73.036 & 58.302 \end{bmatrix} \quad (5.3a)$$

and

$$\mathbf{G} = \begin{bmatrix} 1669.078 & -367.575 & 57.322 & 24.877 \\ 349.498 & 1641.770 & 319.018 & 74.214 \\ -123.294 & -281.404 & 1349.582 & 1004.528 \\ 40.808 & 123.005 & -999.204 & 1381.895 \end{bmatrix}. \quad (5.3b)$$

TABLE II
SIMULATED RESULTS FOR DIFFERENT TRAJECTORIES WHEN $\mathbf{K}$ AND $\mathbf{G}$ ARE GIVEN IN (5.3)

Hold-heating temp. in simulation	Convection effect included			No convection effect		
	$\max_{t\in[0,30]}\max_{i\in[1,101]}\lvert e_i\rvert$	$\min_{t\in[7,30]}\max_{i\in[1,101]}\lvert e_i\rvert$	$\max_{i\in[1,101]}\lvert e_i\rvert\big\rvert_{t=30}$	$\max_{t\in[0,30]}\max_{i\in[1,101]}\lvert e_i\rvert$	$\min_{t\in[7,30]}\max_{i\in[1,101]}\lvert e_i\rvert$	$\max_{i\in[1,101]}\lvert e_i\rvert\big\rvert_{t=30}$
1100℃	0.531	0.213	0.214	0.526	0.210	0.211
1000℃	0.426	0.153	0.153	0.423	0.150	0.152
1200℃	0.642	0.289	0.290	0.636	0.283	0.284

Note that the entries of the gain matrices are much larger than that of the previous case. These control gains are also applied to these cases with different temperature trajectories. Simulations are performed with results shown in Table II. As the results show, the performance is close to that obtained in the previous case. Since the resultant $\mathbf{K}$ and $\mathbf{G}$ give a much higher value of $||Q||_\infty$ ($||Q||_\infty = 299.1618$ while $(1/2\sum_{i=7}^{101}\sigma_i) = 299.8784$), the controller provides a faster response. The tracking errors are driven to steady state more quickly with a smaller peak, $\max_{\substack{1\le i\le 101\\ 0\le t\le 30}} |e_i(t)|$.

VI. CONCLUSIONS AND DISCUSSIONS

This paper proposes a method for RTP temperature control system design. The control system consists of a least square feedforward controller and a feedback controller. It is shown that for RTP systems with typical ramp-up and hold temperature profiles, a simple steady-state reduced order model is adequate for feedback design and very simple PI controller can be used to achieve good temperature tracking, uniformity, and robustness. A method for choosing good temperature sensor locations is also presented.

The design method prespecifies the feedback controller type (PI). With an appropriate choice of performance index, the design reduces to the tuning of two parameters to quantitatively take dynamic performance and robustness into consideration. Systematic and simple tuning procedure is one attribute of the method that is different from RTP design methods proposed in the literature [3], [4], [6], [7], [16]. The simplicity of the PI controller, together with a simple tuning procedure, also makes on-line tuning possible, an advantage in real-time implementation.

Thermal process of RTP, dominated by radiation and conduction, exhibits highly damped and nonoscillatory dynamic response. It thus allows very accurate low-order approximation (the list of Hankel singular values in the example confirms this) and this in turn makes PI control suitable. In general the simplest (decentralized) n-channel multiinput–multioutput (MIMO) PI controller requires $2n$ tuning parameters if the channels are to be independently tuned. In the design example, there are only two parameters for a four-input–four-output system and they seem adequate. The reason is that, for the RTP system, the actuators are all of the same type (lamps) and the performance requirement is dominated by uniformity, thus each channel is of the same importance and hence only two parameters are required. The small number of tuning parameters makes the design approach attractive.

ACKNOWLEDGMENT

The authors would like to thank the reviewers for their comments and suggestions which improved the paper.

REFERENCES

[1] R. B. Fair, *Rapid Thermal Processing: Science and Technology*. New York: Academic, 1993.
[2] P. Singer, "Rapid Thermal Processing: Progress Rep.," Semiconductor International, May 1993.
[3] C. D. Schaper, M. M. Moslehi, K. C. Saraswat, and T. Kailath, "Modeling, identification, and control of rapid thermal processing systems," *J. Electrochem. Soc.*, vol. 141, no. 11, pp. 3200–3209, Nov. 1994.
[4] C. D. Schaper, "Real-time control of rapid thermal processing semiconductor manufacturing equipment," in *Proc. Amer. Contr. Conf.*, June 1993, pp. 2985–2989.
[5] C. D. Schaper, M. Moslehi, K. Saraswat, and T. Kailath, "Control of MMST RTP: Repeatability, uniformity, and integration for flexible manufacturing," *IEEE Trans. Semicond. Manufact.*, vol. 7, pp. 202–219, May 1994.
[6] J. D. Stuber, T. F. Edgar, J. K. Elliott, and T. Breedijk, "Model-based control of rapid thermal process," in *IEEE Proc. 33rd Conf. Decision Contr.*, Dec. 1994, pp. 79–85.
[7] S. Belikov and B. Friedland, "Closed-loop adaptive control for rapid thermal processing," in *Proc. 34th Conf. Decision Contr.*, Dec. 1995, pp. 2476–2481.
[8] C. D. Schaper, T. Kailath, and Y. J. Lee, "Decentralized control of wafer temperature for multizone rapid thermal processing systems," *IEEE Trans. Semicond. Manufact.*, vol. 12, pp. 193–199, May 1999.
[9] J. X. Xu, Y. Chen, T. M. Lee, and S. Yamamoto, "Temperature iterative learning control with application to RTPCVD thickness control," *Automatica*, vol. 35, pp. 1535–1542, 1999.
[10] Y. K. Jan and C. A. Lin, "Lamp configuration design for rapid thermal processing systems," *IEEE Trans. Semicond. Manufact.*, vol. 11, pp. 75–84, Feb. 1998.
[11] Y.-K. Jan, "Lamp Configuration and Control System Design for Rapid Thermal Processing Systems," Ph.D. dissertation, Nat. Chiao-Tung Univ., Hsinchu, Taiwan, R.O.C., 2000.
[12] K. Zbou, F. C. Doyle, and K. Glover, *Robust and Optimal Control*. Englewood Cliffs, NJ: Prentice-Hall, 1995.
[13] B. A. Francis, *Lecture Notes in Control and Information Sciences*. New York: Springer-Verlag, 1987.
[14] T. Kailath, *Linear Systems*. Englewood Cliffs, NJ: Prentice-Hall, 1980.
[15] H. A. Lord, "Thermal and stress analysis of semiconductor wafers in a rapid thermal processing oven," *IEEE Trans. Semicond. Manufact.*, vol. 1, pp. 105–114, Aug. 1988.
[16] P. P. Apte and K. C. Saraswat, "Rapid thermal processing uniformity using multivariable control of a circularly symmetric 3 zone lamp," *IEEE Trans. Semiconduct. Manufact.*, vol. 5, pp. 180–188, Aug. 1992.

Ching-An Lin received the B.S. degree from the National Chiao-Tung University, Taiwan, R.O.C., in 1977, the M.S. degree from the University of New Mexico, Albuquerque, in 1980, and the Ph.D. degree from the University of California, Berkeley, in 1984, all in electrical engineering.

He was with the Chung-Shan Institute of Science and Technology from 1977 to 1979, and with Integrated Systems Inc. from 1984 to 1986. Since June 1986, he has been with the Department of Electrical and Control Engineering, the National Chiao-Tung University, Taiwan, where he is a Professor. His current research interests include multivariable control and signal processing.

Yaw-Kuen Jan received the B.S. degree in electrical engineering from the National Taiwan University, Taiwan, R.O.C., in 1986, and the M.S. degree in control engineering from the National Chiao-Tung University (NCTU), Taiwan, in 1990.

Since 1990, he has been a Vice-Engineer in the Chung-Shan Institute of Science and Technology. He is currently pursuing the Ph.D. degree in control engineering at NCTU, and his research interests are in lamp configuration design and temperature control in rapid thermal processing.